

---



---

## Mechanical Properties IF Steel Processed by ECAP

---



---

### 5.1 Hardness

Figure 5.1 reproduces the variation of hardness with the equivalent strain.

Hardness of as-received IF steel is 175 VHN. At  $\epsilon_{vm}=0.6$  hardness increases to 270 VHN. With increasing strain at 1.2, it enhances to 291 VHN. It increases further to 314 VHN at  $\epsilon_{vm}=1.8$  and reaches 339 VHN at  $\epsilon_{vm}=2.4$ . Thereafter, the rate of hardness improvement decreases with equivalent strain but it continues to increase to about 350 VHN at  $\epsilon_{vm}=24$ .

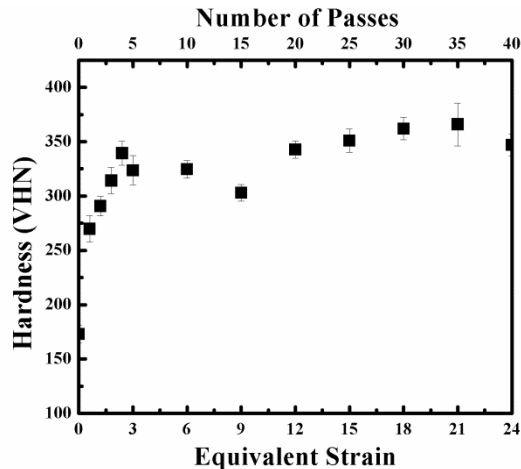


**Figure 5.1:** Variation of yield hardness with equivalent strain.

### 5.2 Tensile Properties

The as-received IF steel has the lowest yield strength of 227 MPa and the ultimate tensile strength of 336 MPa (Figure 5.2(a)). The strength of the steel increases at rapid rate with equivalent strain by ECAP processing. Figure 5.2(b) summarizes the variation of yield strength and ultimate tensile strength with equivalent strain. Yield strength

increases at a rapid rate upto equivalent strain 3. At  $\epsilon_{vm}=3$ , it reaches 710 MPa which is three times to that of the coarse grained counterpart. At  $\epsilon_{vm}=9$ , the yield strength further increases to 842 MPa. Beyond this, at large equivalent strain it increases at slow rate. At  $\epsilon_{vm}=24$  it reaches 895 MPa which is 4 times to that of as-received material. The ultimate tensile strength (UTS) also increases rapidly at low equivalent strain upto  $\epsilon_{vm}=3$  and the difference between yield strength and ultimate tensile strength is lesser than 40 MPa. At  $\epsilon_{vm}=3$ , the UTS becomes 738 MPa which is two and half times that of as-received material. Thereafter, it increases with equivalent strain at slow rate. At  $\epsilon_{vm}=9$  it becomes 898 MPa. But at large equivalent strain ( $\epsilon_{vm}\geq 9$ ) the difference between yield strength and UTS remains in range 40-60 MPa. At large strain  $\epsilon_{vm}=24$ , the ultimate tensile strength becomes 937 MPa which is about 3 times that of as-received IF steel.

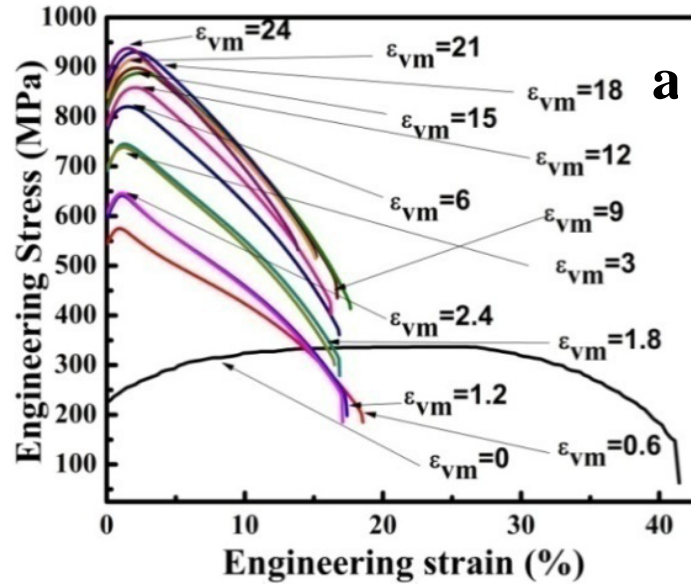


**Figure 5.2:** (a) Engineering stress-strain curves of as-received IF steel and after ECAP for different equivalent (Von Mises') strain ( $\epsilon_{vm}$ )

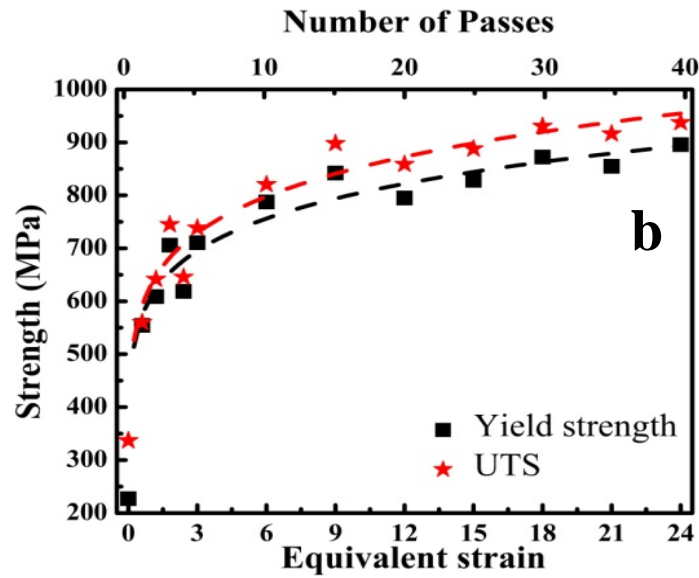


**Figure 5.2:** (b) variation of yield strength and ultimate tensile strength with equivalent strain.

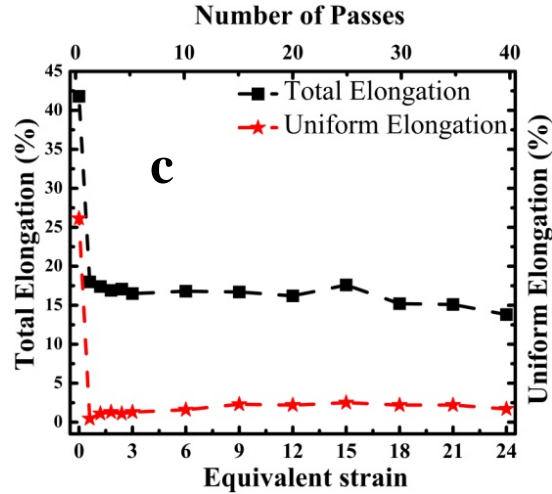


**Figure 5.2:** (c) variation of total elongation and uniform elongation with equivalent strain.

The as-received IF steel has total elongation of 41.8% in which uniform elongation to be of 26.1%. Total elongation reduces drastically from 41% to 18% at  $\epsilon_{vm}=0.6$  (Figure 5.2(c)). Thereafter, it decreases marginally, to 13.8 at  $\epsilon_{vm}=24$ . Uniform elongation also decreases at rapid rate to 0.45% at  $\epsilon_{vm}=0.6$ . It gains marginally about 1%, at  $\epsilon_{vm}=1.2$  and reaches approximately 2% at  $\epsilon_{vm}=9$ . Thereafter it remains unchanged.

### 5.3 Stored Energy

Figure 5.3 provides changes in elastic stored energy with equivalent strain. The as-received hot rolled IF steel shows low elastic stored energy (Figure 5.3). The stored strain energy increases with enhanced equivalent strain and it reaches to 117.3 Joule/mole at  $\epsilon_{vm}=3$ . Thereafter the rate of increase in strain energy decreases though it approaches to a maximum value of 124 Joule/mole at  $\epsilon_{vm}=12$  and remains constant upto  $\epsilon_{vm}=15$ . The stored strain energy drops to 110.6 Joule/mole at  $\epsilon_{vm}=18-21$  and finally it attains a value of 123.6 Joule/mole at  $\epsilon_{vm}=24$ .

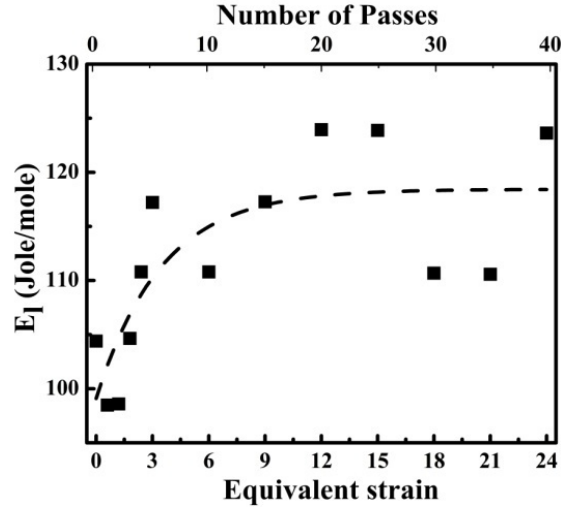


**Figure 5.3:** Variation of elastic strain energy (Joule/mole) with equivalent strain,  $\epsilon_{vm}$ .

#### 5.4 Fractography

Figure 5.5 represents variation of size of dimples with respect to equivalent strain. The fractograph of as-received IF steel reveals presence of large dimples of size  $\sim 60 \mu\text{m}$  (Figure 5.4(a), Figure 5.5). At  $\epsilon_{vm}=0.6$ , the dimple size decreases to  $\sim 38 \mu\text{m}$  (Figure 5.4(b)) & 5.5). The fractographs give signature of the ductile fracture (shown by D) at  $\epsilon_{vm}=0.6-6$  (Figure 5.4(b)-(e)) with decreasing dimple size in general upon increasing  $\epsilon_{vm}$ . At  $\epsilon_{vm}=9$ , the cleavage fracture is also observed (Figure 5.4(e), shown by A). At  $\epsilon_{vm}=12$ , the dimple size further decreases to  $\sim 19.7 \mu\text{m}$  (Figure 5.5). The number of dimples per unit area increases (Figure 5.4(g)) and the amount of cleavage fracture area also increases. At  $\epsilon_{vm}=18$ , voids coalesce by which the size increases to  $\sim 23 \mu\text{m}$  (Figures 5.4(h) & 5.5). Most of the fracture surface looks cleavage type at  $\epsilon_{vm}=21$  (Figure 5.4(i)).

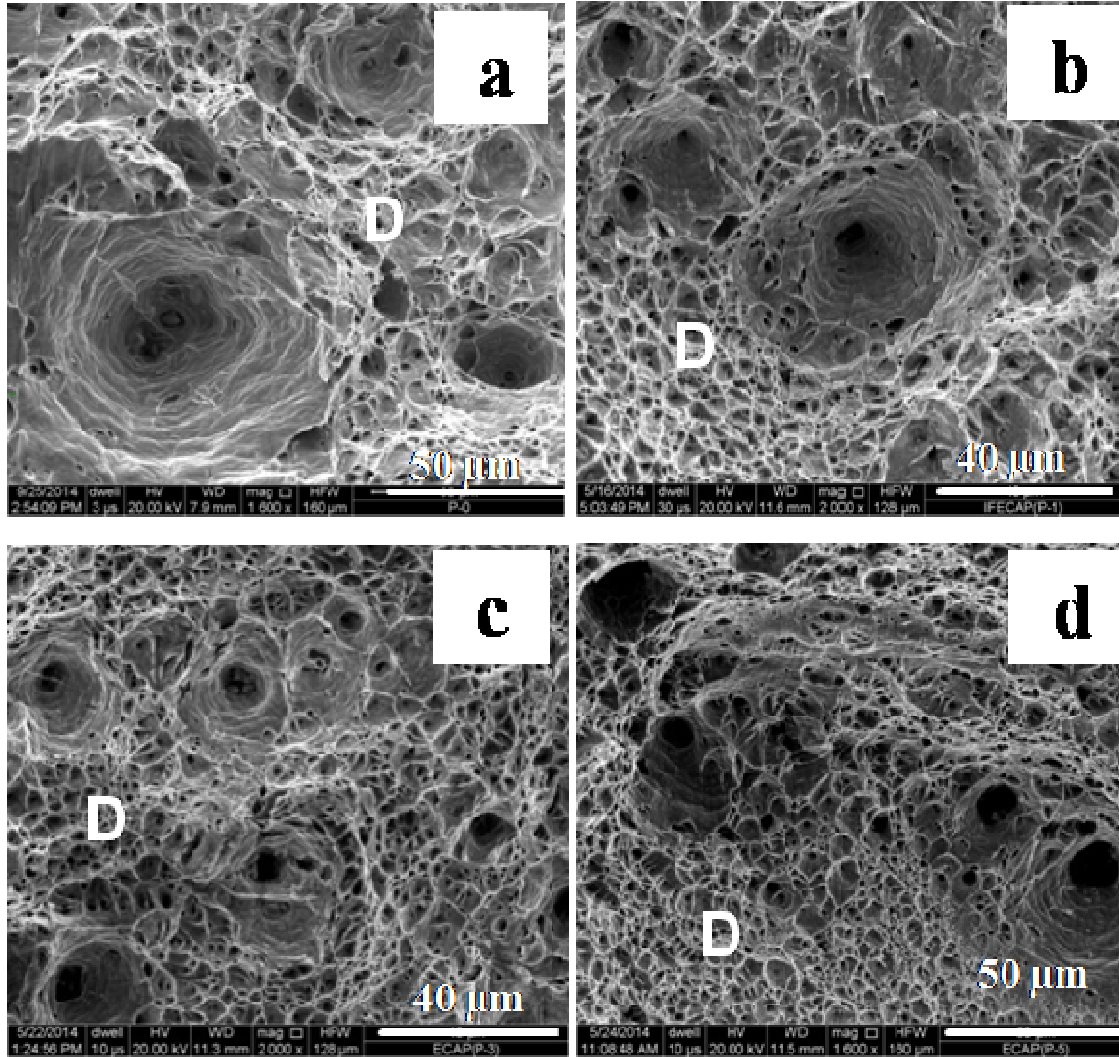


**Figure 5.4:** Microstructure of fracture surface of IF steel of (a) as-received, ECAPed for (b)  $\epsilon_{vm}=0.6$ , (c)  $\epsilon_{vm}=1.8$ , (d)  $\epsilon_{vm}=3$ . D is for dimples or ductile fracture and A stands for cleavage fracture.

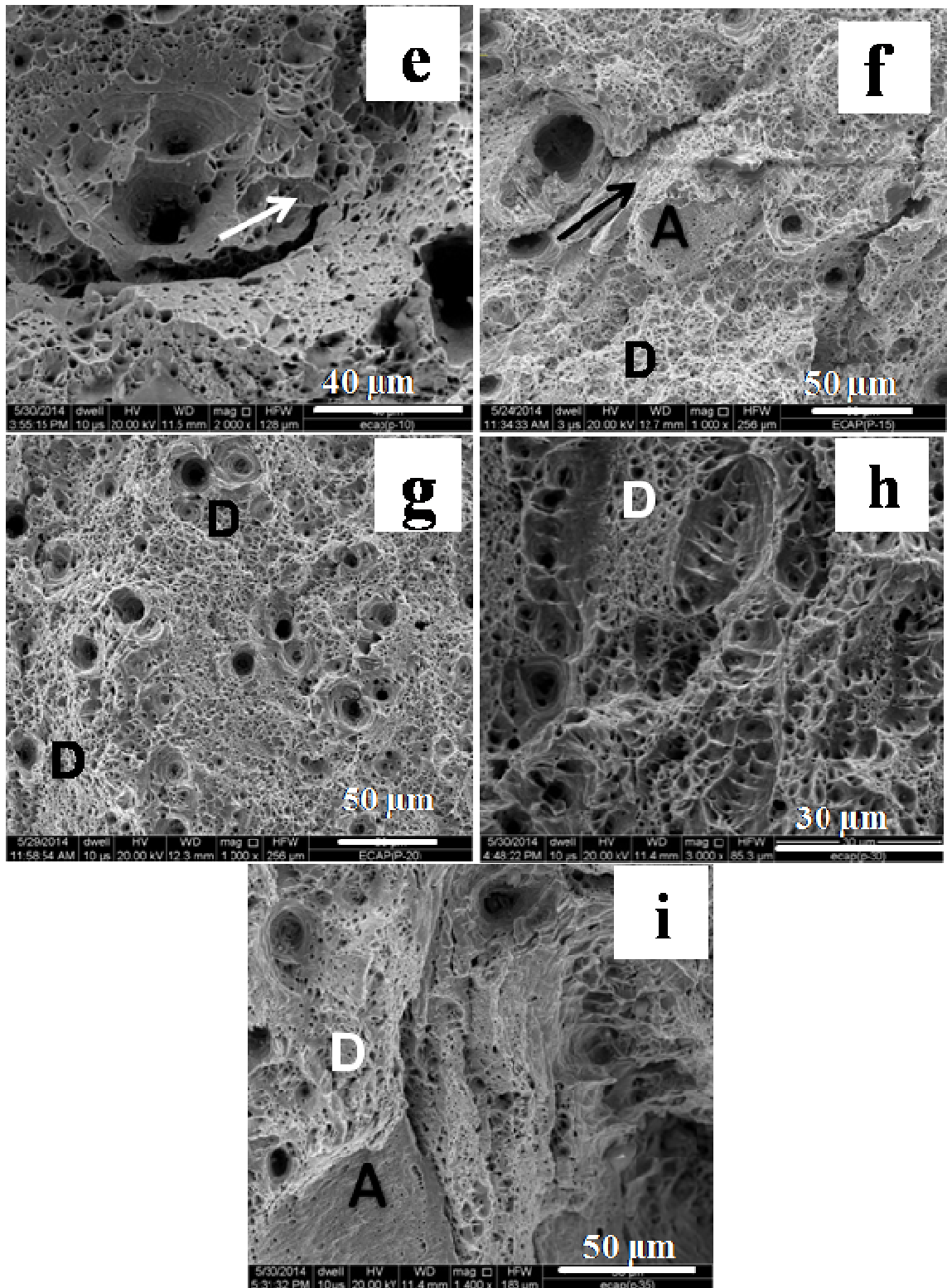


**Figure 5.4:** Microstructure of fracture surface of IF steel of ECAPed for (e)  $\epsilon_{vm}=6$ , (f)  $\epsilon_{vm}=9$ , (g)  $\epsilon_{vm}=12$ , (h)  $\epsilon_{vm}=18$ , (i)  $\epsilon_{vm}=21$ : D is for dimples or ductile fracture and A stands for cleavage fracture.

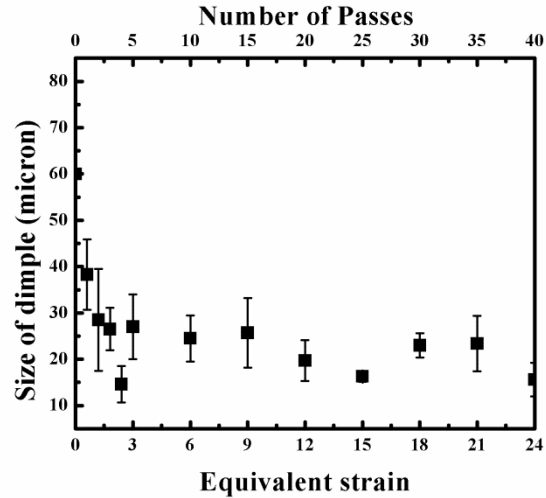


**Figure 5.5:** Variation of size of largest size dimples with equivalent strain,  $\epsilon_{vm}$ .

**Table-5.1:** Details of microstructural parameters and mechanical properties.

$\epsilon_{vm}$	Y.S. (MPa)	U.T.S. (MPa)	T.E. (%)	U.E. (%)	Hardness (VHN)	Dimple size ( $\mu\text{m}$ )	El (J/mole)
0	227	336.7	41.8	26.1	175 $\pm$ 8	60 $\pm$ 10	104.4
0.6	554.5	560	18	0.45	269.7 $\pm$ 12	38.3 $\pm$ 7.6	98.5
1.2	608.6	641.6	17.4	1.1	290.7 $\pm$ 9	28.5 $\pm$ 11	98.5
1.8	705.9	745	16.9	1.3	314.2 $\pm$ 12	26.5 $\pm$ 4.6	104.7
2.4	618.5	645.5	17.0	1.1	339.3 $\pm$ 11	14.6 $\pm$ 3.9	110.8
3	710.5	738.4	16.5	1.3	323.6 $\pm$ 13.5	27 $\pm$ 7	117.2
6	787.4	820.5	16.8	1.6	342.7 $\pm$ 8	24.5 $\pm$ 5	110.8
9	842	898	16.7	2.3	303 $\pm$ 7.6	25.7 $\pm$ 7.5	117.3
12	795	858.7	16.2	2.2	342.7 $\pm$ 8	19.7 $\pm$ 4.4	124
15	828.4	887.8	17.6	2.5	351 $\pm$ 10.9	16.3 $\pm$ 1.2	123.8
18	872.2	930.5	15.2	2.2	362 $\pm$ 10.3	23 $\pm$ 2.6	110.7
21	854.8	916.4	15.1	2.2	366 $\pm$ 19.7	23.4 $\pm$ 6	110.6
24	895.6	937.6	13.8	1.7	347 $\pm$ 10	15.6 $\pm$ 3.6	123.6

Legend: LAGB, M.A., Y.S.=yield strength, U.T.S=universal tensile strength, T.E.=total elongation, U.E.=uniform elongation, TE=total elongation.

## 5.5 Discussion

Coarse grained microstructure ensures the low yield strength as well as the ultimate tensile strength with reasonably high ductility and good work hardening rate (Figure 5.2(a-b)). At equivalent strain of 0.6 the microstructure becomes banded with high trapped dislocation density. The grain refinement with high defect density ensures a sharp increase in the yield strength as well as the tensile strength. At  $\varepsilon_{vm}=1.8-3$ , significant amount of recovery occurs. Therefore strengthening rate with respect to equivalent strain above 3, goes down even though at later stage, the grain size decreases and grain boundary misorientation angle increases with strain. Both the decrease in grain size and increase in misorientation angle together are able to overcome softening due to the recovery of dislocations and to strengthen the material almost at constant rate with respect to the equivalent strain even beyond  $\varepsilon_{vm}=9$  and upto  $\varepsilon_{vm}=24$  (Figure 5.2(a) & (b)) [Purcek 2012, Saray 2013, Iwahashi 1998, Gazder 2008, Saray 2010, Krajňák 2013, Gazder 2008, Máthis 2011, Saray 2012].

The total elongation and the uniform elongation (Figure. 5.2(c)) of as-received IF steel are high due to relatively coarse grained structure. At  $\varepsilon_{vm}=0.6$ , the microstructure becomes banded with high density of trapped dislocations. The ductility drastically drops down due to early necking that results because of low work hardening rate [Saray 2010] which is attributed to low density of mobile dislocations. The total elongation reduces to 18% and the uniform elongation to 0.45% at  $\varepsilon_{vm}=0.6$ . With increasing equivalent strain, the total elongation decreases marginally (1-2%) but uniform elongation improves about 1.5-2% upto equivalent strain of 9, thereafter it remains unchanged while structure is near-equiaxed at large strain 9-24. This increase in elongation is attributed to the

reduction in dislocation density and increase in the HAGB fraction. Hardening behavior (Figure 5.1) with equivalent strain is very similar to strengthening of the steel. At low equivalent strain of 0-2.4, the hardness increases rapidly due to increase in dislocation density and decrease in grain size. But there after the dislocation recovery process occurs. Therefore, the hardness decreases at  $\epsilon_{vm}=3-9$ , whereas at  $\epsilon_{vm}=9-24$  the hardness improves due to the increase in misorientation angle (Figure 3.5).

Stage I which is work hardening due to activation of single slip system is missing in this ECAP processed material. Stage II which is associated with onset of multiple slip and strong work hardening resulting from interactions among dislocations on nonparallel planes starts immediately after yielding that results in linear increase in strength. Stage III which is a recovery stage show reduced work hardening rate at the onset and thereafter at high strain, work hardening is balanced by the recovery processes that gives nearly zero slope (flat region).

At  $\epsilon_{vm}=0.6-1.2$ , strength increases because of significant work hardening and fragmentation of grains to bands by virtue of this further dislocation mediation becomes difficult. This feature is indicated in Figure 5.2a. The similar work hardening rate continues upto  $\epsilon_{vm}=12$ . The slope II strengthening decreases from  $\epsilon_{vm}=15$  onwards. In  $\epsilon_{vm}=0.6-6$ , stage III is missing where recovery processes are restricted. Beyond  $\epsilon_{vm}=6$ , there are two stages in stage III of work hardening behavior of ECAPed IFsteel. At onset of stage III, recovery processes begin under tensile loading and after significant recovery rate strengthening is counter balanced by rate of recovery and thereby slope of tensile curve decreases to nearly zero. Rate of recovery is more with increase in  $\epsilon_{vm}$ . Beyond  $\epsilon_{vm}=9$ , it shows that the microstructure is stabilized by various recovery processes. Both

the decrease in grain size and increase in misorientation angle together are able to strengthen the material almost at constant rate with respect to the equivalent strain even beyond  $\epsilon_{vm}=9$  and upto  $\epsilon_{vm}=24$  (Figure 5.2(a) & (b)).

As-received IF steel has low elastic stored energy and large size dimples in fractured surface, which are indicative of high ductility for the material. The dimple size decreases with the increase of  $\epsilon_{vm}$  from 0.6 to 6 (Figure 5.4(b)-(e)) due to the higher stored strain energy (Figure 5.4(b)) and the increased fraction of LAGBs (Figure 3.5(a)). Energy required for nucleation of dimples is more than that of their growth and coalescence [Tarpani 2002]. At an equivalent strain range of  $\epsilon_{vm}=6-9$  (Figure 5.4(e)-(f)), the elastic stored energy remains nearly constant and size of dimples are also comparable but the depth of the dimples get reduced (visual observation in Figure 5.4(e)-(f)). Fractographs (Figure 5.4(e) and (f)) show that the fracture is initiated in the transverse direction (perpendicular to the axes of tensile testing as shown by arrow). Moreover, the minimization of depth of the dimples is ascribed to the reduction in ductility [Dieter 1988, Hertzberg 2011, Callister 2010, Raghavan 2010]. At large equivalent strain,  $\epsilon_{vm}=9$  (Figure 5.4(f)), the cleavage fracture [Dieter 1988, Hertzberg 2011, Callister 2010, Raghavan 2010] can be observed (marked by A). The amount of cleavage fracture area increases with the equivalent strain ranging from 9 to 24 (Figure 5.4(g)-(i)). At  $\epsilon_{vm}=12$ , the inhomogeneity in microstructure (Figure 5.4(g)) is observed, as both the type of grains, i.e. the ribbon shaped as well as the nearly equiaxed ultrafine grains coexist. Due to continuous straining, more strain energy is accumulated, the number of dimples per unit area increases and dimples become deeper (Figure 5.4(g)), there by the uniform

elongation is maintained. At  $\epsilon_{vm}=21$ , the majority of the areas are failed by the cleavage fracture (marked by A in Figure 5.4(i)) indicating limited ductility.

## 5.6 Summary

Both the yield strength and the ultimate tensile strength increase sharply upto  $\epsilon_{vm}=3$  due to the rapid microstructural refinement with high defect density. Thereafter, the strength increases appreciably upto  $\epsilon_{vm}=9$  as LAGB fraction decreases and average misorientation angle increases. The strengthening continues to occur even upto  $\epsilon_{vm}=24$ , as the increase in high angle grain boundary fraction and average misorientation angle take place although the grain refinement at  $\epsilon_{vm}$  greater than 9 is not significant. The strengthening of the selected interstitial-free steel showing yield strength 227 MPa to 895 MPa by ECAP for  $\epsilon_{vm}=24$  at 298K is itself noteworthy. The uniform elongation of the IF steel reduces to 0.5% by ECAP due to a lack of work hardening ability at a low strain level ( $\epsilon_{vm}=0.6$ ). With increasing strain the elongation improves marginally by 1.5-2% upto  $\epsilon_{vm}=9$ , and there after it remains almost constant. The ECAPed sample fails by ductile fracture at lower range of  $\epsilon_{vm}=0.6-6$  but by the mixed mode of ductile-brittle fracture at larger equivalent strain (9-24).